

## Supporting Information

### Theranostic CuS Nanoparticles Targeting Folate Receptors for PET Image-Guided Photothermal Therapy

Min Zhou<sup>a,b,#</sup>, Shaoli Song<sup>a, c,#</sup>, Jun Zhao<sup>a</sup>, Mei Tian<sup>b</sup>, Chun Li<sup>a,\*</sup>

<sup>a</sup>Department of Cancer Systems Imaging, The University of Texas MD Anderson Cancer Center, Houston, Texas 77054, United State.

<sup>b</sup>The Second Hospital of Zhejiang University, Hangzhou, Zhejiang, China

<sup>c</sup>Department of Nuclear Medicine, Renji Hospital, Shanghai Jiaotong University School of Medicine, Shanghai 200127, P. R. China

#### **\*Corresponding Author:**

Chun Li, Department of Cancer Systems Imaging, Unit 1907, The University of Texas MD Anderson Cancer Center, Houston, Texas 77030; Phone: (713) 792-5182; Fax: (713) 794-5456; E-mail: cli@mdanderson.org.

<sup>#</sup>These authors contributed equally to this work

## Table of Contents

- Figure S1:** Zetal potential analysis of FA-CuS NPs.
- Figure S2.**  $^1\text{H}$  NMR analysis of FA-CuS NPs
- Figure S3.** Temperature change curve of FA-CuS NPs under NIR laser irradiation at 1.5 W/cm<sup>2</sup>.
- Figure S4.** Dynamic light scattering (DLS) of FA-CuS NPs in PBS or FBS solution
- Figure S5.** Radiolabeling efficiency of FA-[<sup>64</sup>Cu]CuS NPs
- Figure S6.** Comparison of the UV-vis spectra of FA-CuS NPs and FA-[<sup>64</sup>Cu]CuS NPs
- Figure S7.** Dynamical light scattering (DLS) of FA-[<sup>64</sup>Cu]CuS NPs
- Figure S8.** Stability of FA-[<sup>64</sup>Cu]CuS NPs
- Figure S9.** Biodistribution of FA-[<sup>64</sup>Cu]CuS NPs in orthotopic HeyA8 ovarian tumor model

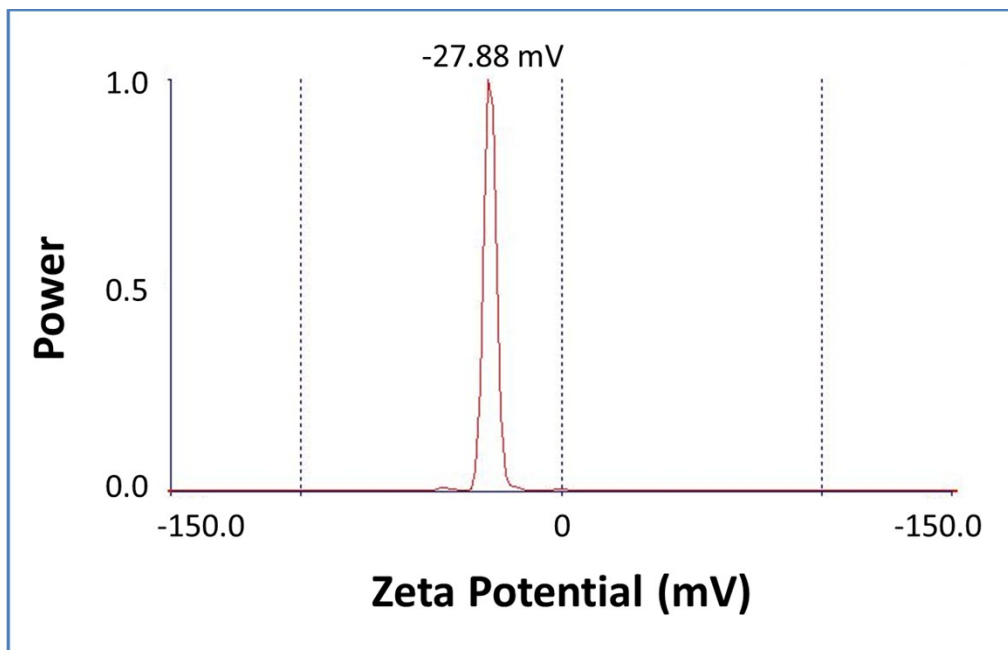
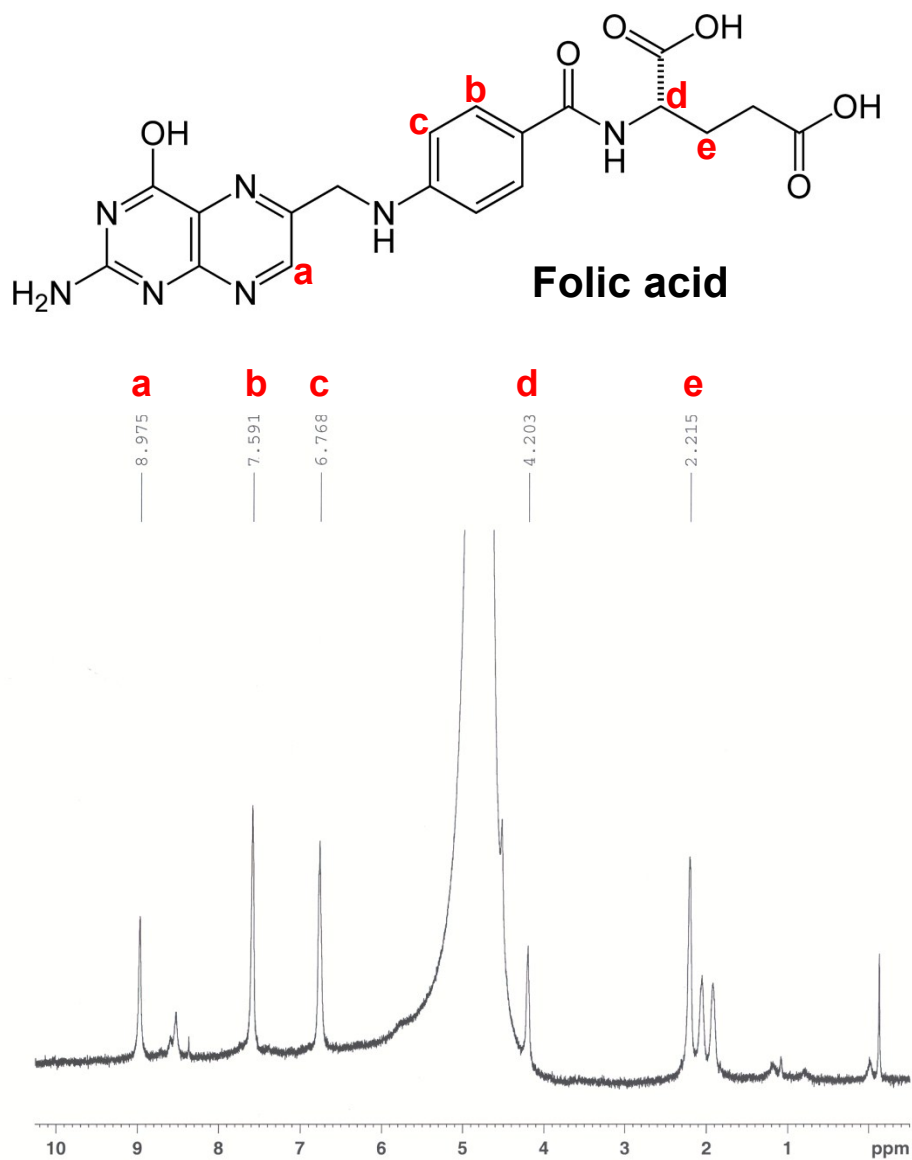


Figure S1: Zetal potential analysis of FA-CuS NPs.



**Figure S2. <sup>1</sup>H NMR analysis of FA-CuS NPs.** The typical peaks of FA at 8.98, 7.59, 6.76, 4.20, and 2.22 ppm representative of FA molecules were observed in the spectrum acquired with purified FA-CuS NPs, indicating FA molecules were successfully coated to the surface of CuS NPs.

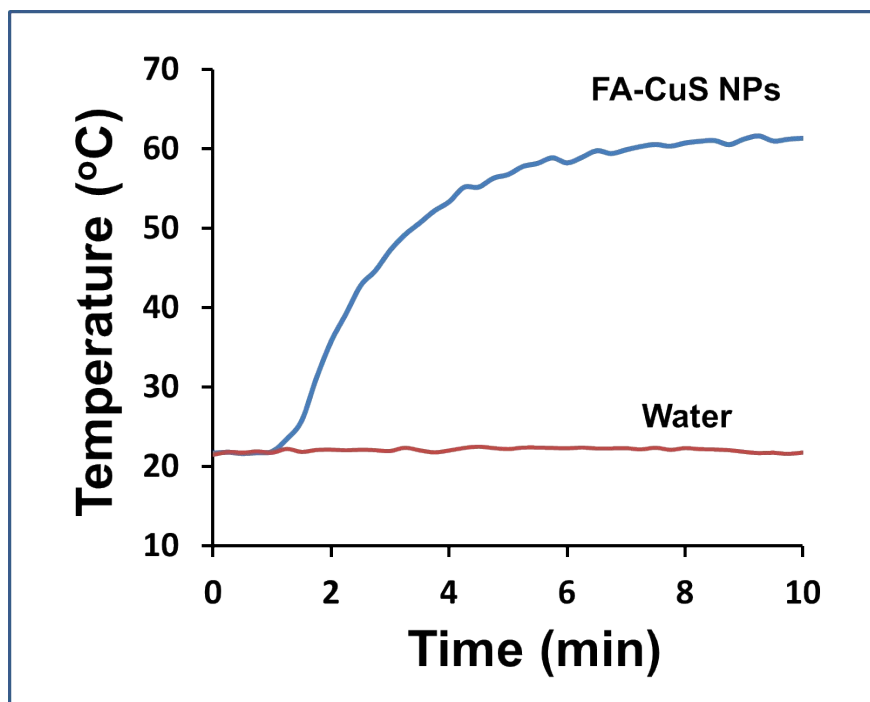
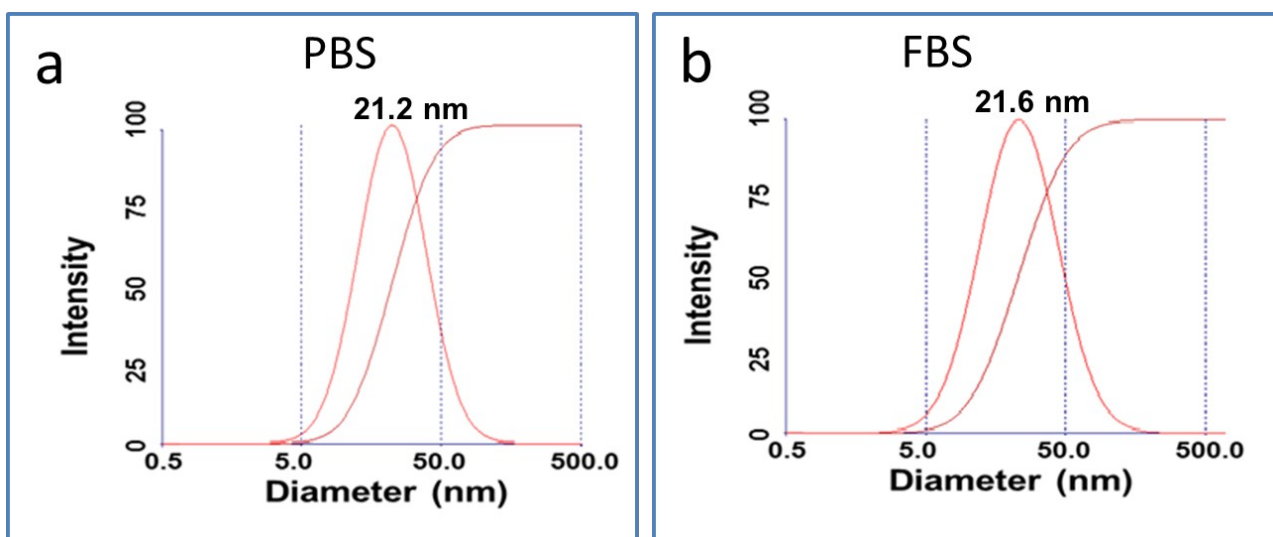
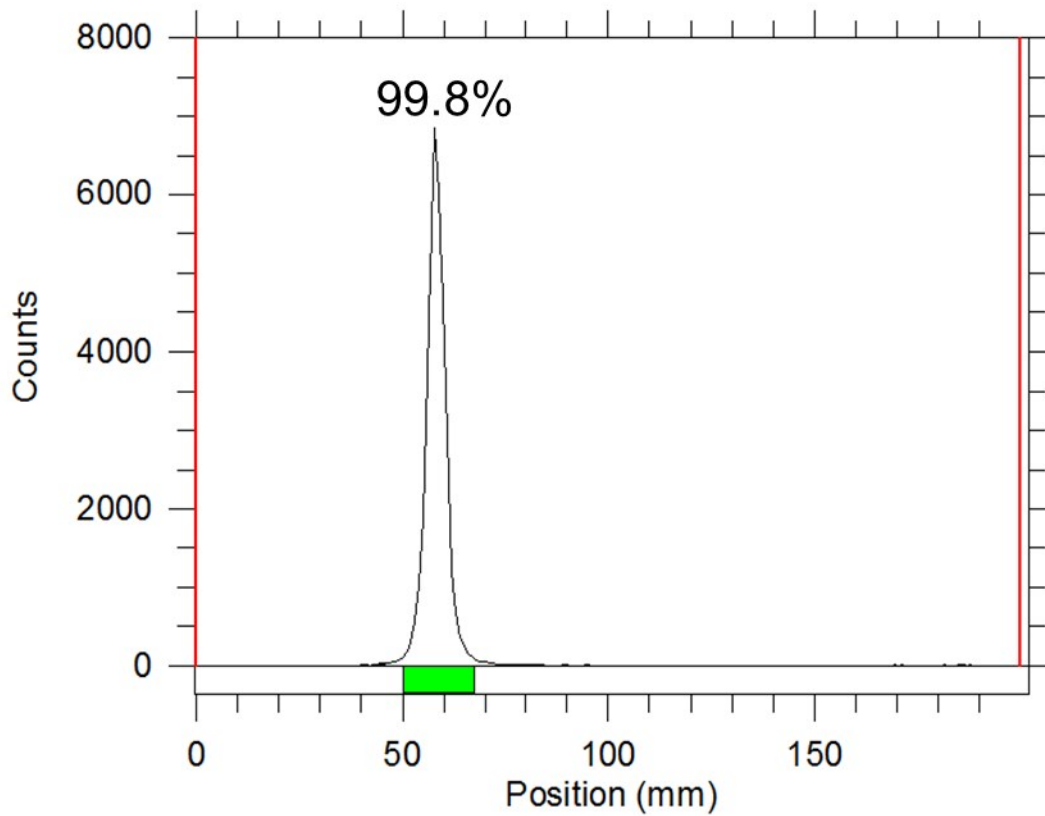


Figure S3. Temperature change curve of FA-CuS NPs (100  $\mu\text{g}/\text{mL}$ ) under NIR laser irradiation (808 nm, 1.5  $\text{W}/\text{cm}^2$ ).



**Figure S4.** Dynamic light scattering (DLS) of FA-CuS NPs in PBS or PBS containing 10% FBS at 37°C for up to 7 days.



**Figure S5. Radiolabeling efficiency of FA-<sup>64</sup>Cu]CuS NPs.** Greater than 99% of the radioactivity was associated with FA-<sup>64</sup>Cu]CuS NPs at the end of synthesis.

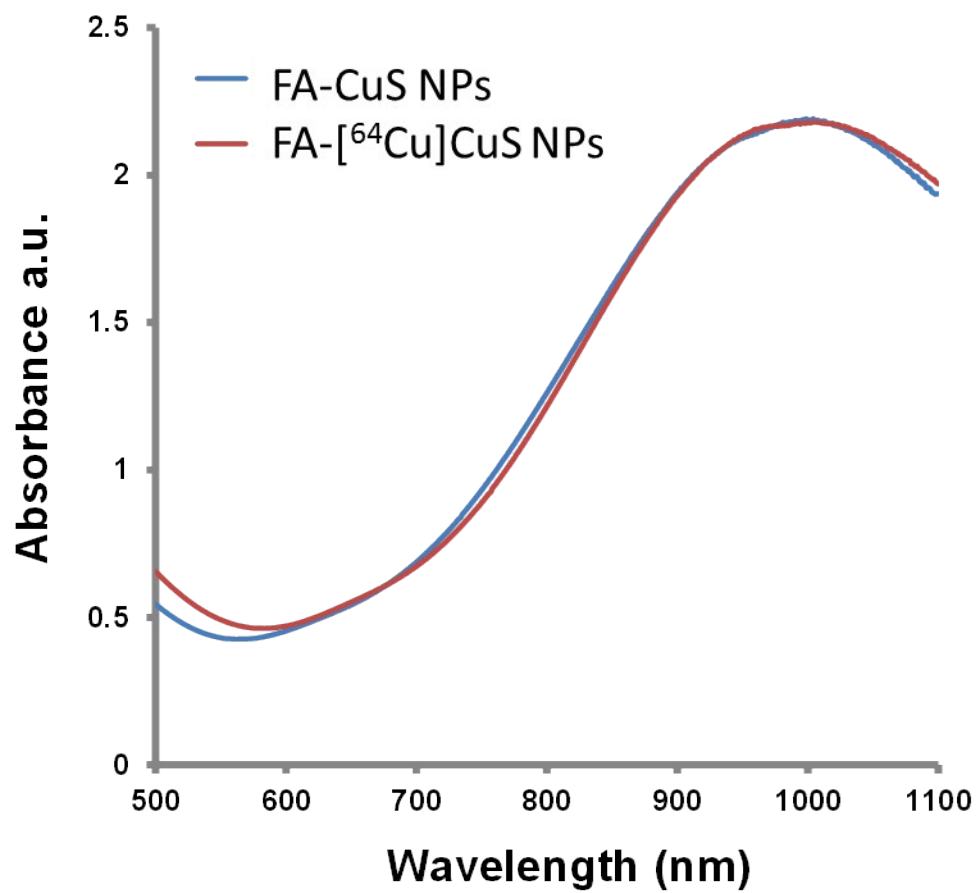


**Figure S6. Comparison of the UV-vis spectra of FA-CuS NPs and FA-[<sup>64</sup>Cu]CuS NPs.** FA-[<sup>64</sup>Cu]CuS NPs correlated well with the spectroscopic features observed for the non-radioactive FA-CuS NPs, indicating similarity between the two NPs at the tracer and macroscopic levels.

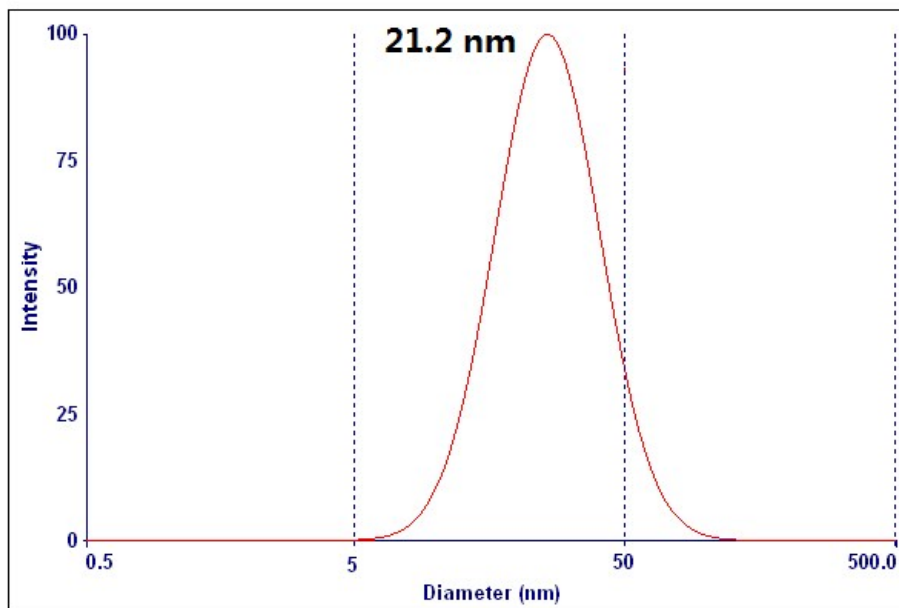


**Figure S7. Dynamical light scattering (DLS) of FA-[<sup>64</sup>Cu]CuS NPs.** The hydrodynamic diameter of the FA-[<sup>64</sup>Cu]CuS NPs is 21.2 nm. There is no significant difference with the non-radioactive FA-CuS NPs (21.0 nm).

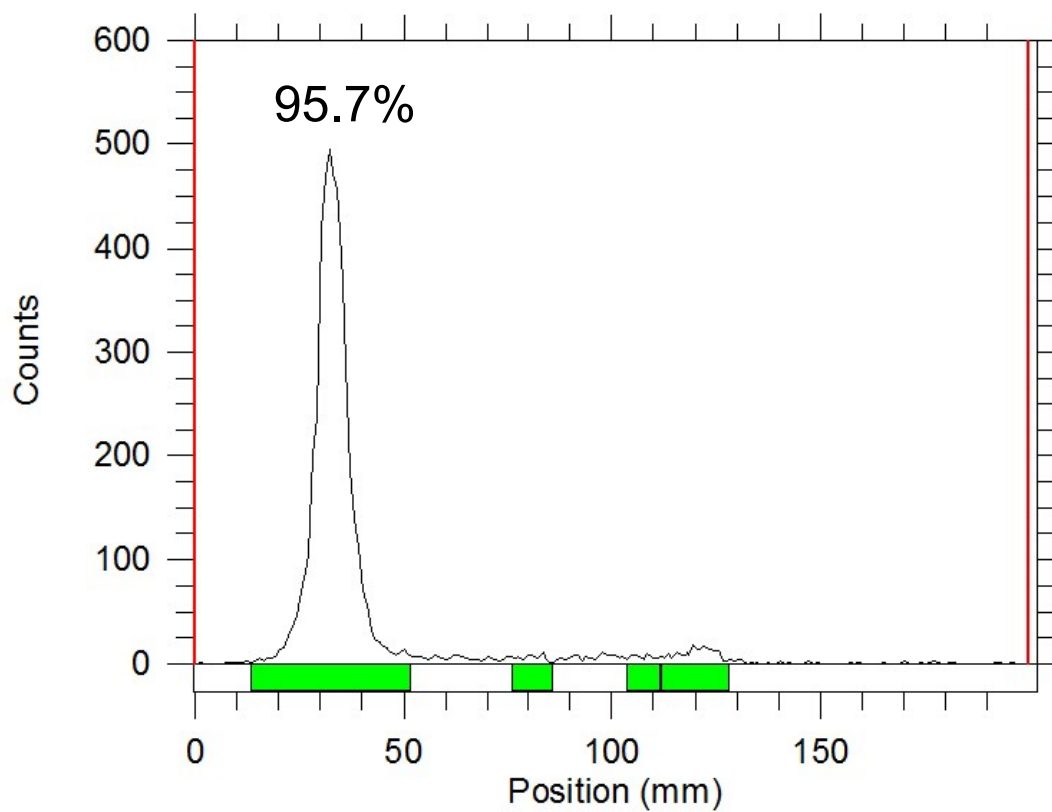


**Figure S8. Stability of FA- $^{64}\text{Cu}$ ]CuS NPs.** After incubation in 10% FBS-PBS solution at 37°C for 24 h, less than 5% of radioactivity was dissociated from FA- $^{64}\text{Cu}$ ]CuS NPs.

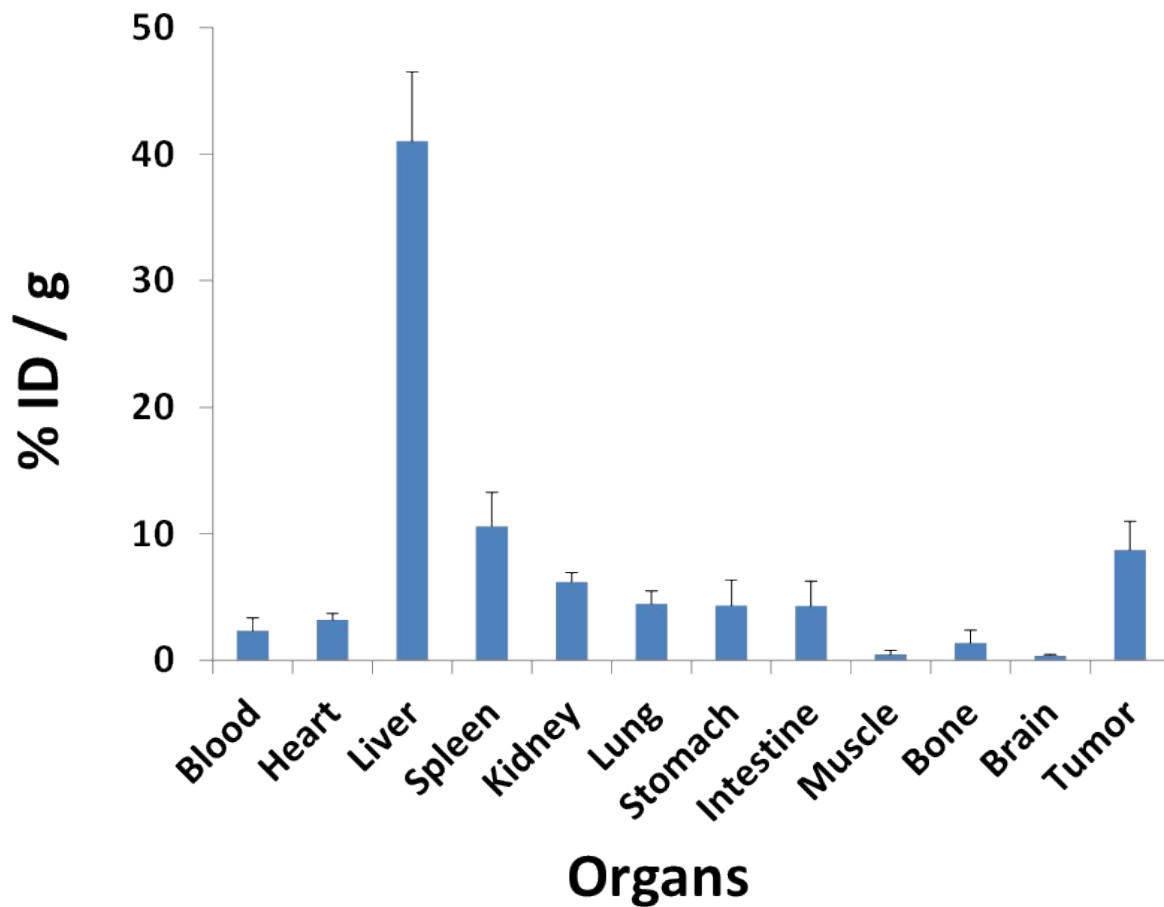


**Figure S9. Biodistribution of FA-[<sup>64</sup>Cu]CuS NPs in orthotopic HeyA8 ovarian tumor model.**

Female nude mice were inoculated with HeyA8 cells intraperitoneally ( $1 \times 10^6$  cells/mouse). At 20 days after tumor inoculation, mice were injected with FA-[<sup>64</sup>Cu]CuS NPs intravenously (200  $\mu$ Ci/mouse). Mice were killed at 24 h after NP injection, and various tissues were removed for radioactivity counting. The data are presented as mean  $\pm$  standard deviation (n = 6).